



Published in final edited form as:

Kidney Int. 2022 April ; 101(4): 711–719. doi:10.1016/j.kint.2021.10.036.

Enteral ferric citrate absorption is dependent on the iron transport protein ferroportin

Mark R. Hanudel¹, Brian Czaya², Shirley Wong², Maxime Rappaport¹, Shweta Namjoshi¹, Kristine Chua², Grace Jung², Victoria Gabayan², Bo Qiao², Elizabeta Nemeth², Tomas Ganz²

¹Department of Pediatrics, David Geffen School of Medicine at UCLA, Los Angeles, California, USA

²Department of Medicine, David Geffen School of Medicine at UCLA, Los Angeles, California, USA

Abstract

Ferric citrate is approved as an iron replacement product in patients with non-dialysis chronic kidney disease and iron deficiency anemia. Ferric citrate-delivered iron is enterally absorbed, but the specific mechanisms involved have not been evaluated, including the possibilities of conventional, transcellular ferroportin-mediated absorption and/or citrate-mediated paracellular absorption. Here, we first demonstrate the efficacy of ferric citrate in high hepcidin models, including *Tmprss6* knockout mice (characterized by iron-refractory iron deficiency anemia) with and without adenine diet-induced chronic kidney disease. Next, to assess whether or not enteral ferric citrate absorption is dependent on ferroportin, we evaluated the effects of ferric citrate in a tamoxifen-inducible, enterocyte-specific ferroportin knockout murine model (*Villin-Cre-ERT2*, *Fpn^{flox/flox}*). In this model, ferroportin deletion was efficient, as tamoxifen injection induced a 4000-fold decrease in duodenum ferroportin mRNA expression, with undetectable ferroportin protein on Western blot of duodenal enterocytes, resulting in a severe iron deficiency anemia phenotype. In ferroportin-deficient mice, three weeks of 1% ferric citrate dietary supplementation, a dose that prevented iron deficiency in control mice, did not improve iron status or rescue the iron deficiency anemia phenotype. We repeated the conditional ferroportin knockout experiment in the setting of uremia, using an adenine nephropathy model, where three weeks of 1% ferric citrate dietary supplementation again failed to improve iron status or rescue the iron deficiency anemia phenotype. Thus, our data suggest that enteral ferric citrate absorption is dependent on conventional enterocyte iron transport by ferroportin and that, in these models, significant paracellular absorption does not occur.

Keywords

ferric citrate; ferroportin; hepcidin; iron; anemia; chronic kidney disease

*Correspondence: Mark Hanudel, UCLA Department of Pediatrics, Division of Pediatric Nephrology, 10833 Le Conte Avenue, MDCC A2-383, Los Angeles, California 90095-1752, USA. mhanudel@mednet.ucla.edu.

SUPPLEMENTARY MATERIAL
Supplementary File (Word)

Auryxia (ferric citrate [FC]; Akebia Therapeutics, Inc., Cambridge, MA) is a novel compound that is approved for clinical use as an enteral phosphate binder in adult chronic kidney disease (CKD) patients on dialysis. In randomized, placebo-controlled trials conducted in non-dialysis-dependent CKD patients, FC significantly decreased serum phosphate concentrations.^{1,2} In randomized, active-controlled trials conducted in dialysis-dependent CKD patients, FC produced similar reductions in serum phosphate concentrations.^{3,4}

Auryxia is also approved in the US for clinical use as an iron-replacement product in CKD non-dialysis patients with iron-deficiency anemia. In the 4 aforementioned randomized controlled trials, conducted in both non-dialysis-dependent and dialysis-dependent CKD cohorts, FC significantly increased serum transferrin saturation (TSAT).¹⁻⁴ Thus, FC can function as both an effective enteral phosphate binder and an enteral iron source.

It is remarkable that FC corrects iron deficiency in the setting of CKD, and even end-stage renal disease, as these are states with high hepcidin levels.⁵⁻⁸ Hepcidin is the master iron-regulatory hormone, binding to and inhibiting ferroportin, the only known cellular iron exporter.⁹ In the setting of high hepcidin levels, the activity of ferroportin—located on the basal surface of enterocytes—is decreased, thus inhibiting dietary and medicinal iron absorption from the gastrointestinal lumen (Figure 1¹⁰).

The mechanisms by which FC overcomes the enteral iron block induced by high hepcidin and low ferroportin levels are unclear. One hypothesis is that the citrate moiety in FC chelates calcium ions, leading to disruption of enterocyte intercellular tight junctions, allowing for paracellular iron absorption that is independent of the hepcidin-ferroportin pathway. An interesting point to note is that citrate compounds have been noted to facilitate paracellular enteral absorption of aluminum,^{11,12} raising the possibility that iron absorption is enhanced by the same mechanism. In order to assess whether FC-associated enteral iron absorption occurs via a transcellular, ferroportin-dependent route, versus a paracellular, ferroportin-independent route, we evaluated enteral FC absorption in murine models, with or without CKD, with low or absent enterocyte ferroportin activity.

METHODS

Mouse experiments

Experiments were conducted in accordance with University of California, Los Angeles (UCLA) Division of Laboratory Animal Medicine guidelines, and the study protocols were approved by the UCLA Office of Animal Research Oversight. Mice were housed at UCLA, in standard cages with wood-chip bedding that was changed twice weekly. Animal housing rooms were temperature and humidity controlled, with a 12-hour light cycle. We first assessed the effects of FC in transmembrane serine protease 6 (*Tmprss6*) knockout mice, a model characterized by high hepcidin levels, low ferroportin activity, and resultant iron-refractory iron-deficiency anemia,¹³ both without and with the addition of adenine diet-induced CKD, which further increases hepcidin levels.¹⁴ To completely inhibit enteral ferroportin activity, we next assessed the effects of FC in a tamoxifen-inducible, enterocyte-specific ferroportin (FPN) knockout model (Villin-Cre-ER^{T2}, *Fpn*^{flox/flox}). Finally, we

assessed the effects of FC in a Villin-Cre-ER^{T2}, Fpn^{flox/flox} model with adenine diet-induced CKD.

***Tmprss6* knockout mice**

Tmprss6 knockout mice on a C57BL/6 genetic background were kindly provided by Dr. Jodie Babitt (Massachusetts General Hospital). We first assessed the effects of FC in *Tmprss6* knockout mice and wild-type (WT) littermates without CKD. Mice aged 4–7 weeks were fed 50 ppm iron diets without adenine (Envigo, Hackensack, NJ), with or without 0.1% FC (Akebia Therapeutics, Inc.), for 3 weeks, and then were euthanized. We next assessed the effects of FC in *Tmprss6* knockout mice and WT littermates with CKD. Mice aged 8–12 weeks were fed 50 ppm iron diets with 0.2% adenine (Envigo) to induce CKD,^{15–17} for 6 weeks. For the last 3 weeks of the diets, 0.1% FC (Akebia Therapeutics, Inc.) was added for one group and not added for another. This FC dose in mice corresponds to a typical adult human FC dose; in an adult human, 2 Auryxia tablets taken thrice daily (6000 mg FC) contain a cumulative daily ferric iron dose of 1260 mg, an amount equivalent to approximately one-third of total body iron. In mice, approximately one-third of total body iron is equivalent to ~0.8 mg of ferric iron daily, or ~4 mg of FC daily which, given murine daily food consumption of ~4 g, corresponds to chow containing 0.1% FC. In these experiments, each group contained approximately half males and half females. After sacrifice, we collected whole blood, serum, liver, and duodenal enterocytes. To isolate duodenal enterocytes, the proximal section of the duodenum (~2 cm) was cut open lengthwise and transferred to ice-cold ethylenediamine tetraacetic acid solution. The solution was vortexed to facilitate cell detachment, and the dispersed cells were collected by filtration.

Non-CKD enterocyte-specific ferroportin knockout mice

Tamoxifen-inducible, enterocyte-specific ferroportin (FPN) knockout mice were generated by breeding Villin-Cre-ER^{T2} mice with Fpn^{flox/flox} mice, both of which are on C57BL/6 genetic backgrounds. Villin-Cre-ER^{T2} mice were kindly provided by Dr. Peter Tontonoz (UCLA). To characterize this model, we assessed Fpn^{flox/flox} mice, with or without Villin-Cre-ER^{T2}, with or without tamoxifen induction (0.075 mg/g body weight, injected i.p. once daily for 4 consecutive days; Sigma-Aldrich, St. Louis, MO). To assess the effects of FC in this model, we used Villin-Cre-ER^{T2}, Fpn^{flox/flox} mice aged 6–8 weeks that were i.p. injected with either sunflower oil vehicle (uninduced group) or tamoxifen (0.075 mg/g body weight; induced group) once daily for 4 consecutive days. Mice were maintained on 50 ppm iron diets (Envigo), and then were euthanized 7 weeks post-injection. Some of the tamoxifen-induced mice had 1% FC added to their diets for the 3 weeks immediately prior to sacrifice. In these experiments, 1% FC—a supraphysiologic dose—was chosen so as not to miss an effect secondary to insufficient FC dosing. To demonstrate the efficacy of this dose, we performed a separate positive control experiment in which we assessed whether 3 weeks of 1% FC dietary supplementation can rescue the iron-deficiency anemia phenotype in uninduced Villin-Cre-ER^{T2}, Fpn^{flox/flox} mice fed a low-iron (4 ppm) diet (Envigo). In the non-CKD enterocyte-specific ferroportin knockout experiments, each group contained both males and females. After sacrifice, we collected whole blood, serum, liver, duodenal enterocytes, and whole duodenum for iron staining. Duodenal enterocytes were isolated

as described above. For duodenal iron staining, proximal duodenal samples were fixed in formalin, then embedded in paraffin blocks from which slides were created. Deparaffinized sections were stained with the Perls Prussian blue stain for nonheme iron and counterstained with nuclear fast red. The degree of duodenal enterocyte iron staining was assessed on a semi-quantitative scale by a blinded reviewer (SN).

CKD enterocyte-specific ferroportin knockout mice

To repeat the above experiment in the setting of CKD, male Villin-Cre-ER^{T2}, Fpn^{flox/flox} mice aged 6 weeks were started on 0.2% adenine diets (Envigo) to induce CKD. Given gender differences in the adenine diet-induced rodent CKD model (females are more resistant to the effects of dietary adenine),¹⁸ only male mice were used. At age 8 weeks, mice were i.p. injected, as described above, with sunflower oil vehicle or tamoxifen. At age 12 weeks, after 6 weeks of the adenine diet, mice were switched to standard, non-adenine, 50 ppm iron diets with or without 1% FC added. Mice were sacrificed at age 15 weeks, 7 weeks post-injection, and after 3 weeks of treatment with or without FC. Whole blood, for hemoglobin and red blood cell measurement, was collected when mice were aged 8 weeks (at the time of injection), 12 weeks (upon initiation of diets with or without FC), and 15 weeks (at sacrifice). Serum, for urea nitrogen and iron measurement, was collected when mice were aged 12 and 15 weeks. Liver and duodenal enterocytes were collected, as described above, at sacrifice.

Blood assays

Complete blood counts were measured by the Hemavet 950 automated processor (Drew Scientific, Oxford, CT). Colorimetric methods were used to assay serum urea nitrogen (BioAssay Systems, Hayward, CA) and serum iron (Genzyme, Cambridge, MA). In-house enzyme-linked immunosorbent assays (ELISA) were used to measure serum hepcidin level, as previously described.¹⁹ A commercially available ELISA kit was used to measure serum erythropoietin (R&D Systems, Minneapolis, MN).

Quantitative liver iron concentrations

Harvested livers were snap-frozen in liquid nitrogen and stored at -80 °C. Small pieces of the livers (~100 mg) were weighed and homogenized. Protein precipitation solution (0.53 N HCl and 5.3% trichloroacetic acid in double-distilled water) was added, and the samples were boiled and centrifuged. Iron concentrations in the supernatants were measured by a colorimetric assay (Genzyme), then normalized to the weights of the original samples to yield tissue iron concentrations.

Quantitative real-time polymerase chain reaction (PCR)

Duodenal enterocytes were homogenized in Trizol (Invitrogen, Waltham, MA), and RNA was isolated according to the manufacturer's protocol. We performed quantitative reverse transcription (RT)-PCR using the iScript RT-PCR kit (Bio-Rad, Hercules, CA) and primers specific for mouse *Fpn* (forward: 5'-ATGGGAAGTGTGGCCTTAC-3'; reverse: 5'-TCCAGGCATGAATACGGAGA-3'). We used the following PCR conditions: initial denaturation at 95 °C for 2 minutes, followed by 40 cycles of

denaturation at 94 °C for 30 seconds, annealing at 58 °C for 30 seconds, extension at 72 °C for 1 minute, and final extension at 72 °C for 10 minutes. Gene expression was normalized to that of hypoxanthine–guanine phosphoribosyltransferase (*Hprt*) (forward: 5'-CTGGTTAAGCAGTACAGCCCCAA-3'; reverse: 5'-CAGGAGGTCCTTTTACCAGC-3'), and each RNA sample was analyzed in duplicate. Relative fold gene expression was calculated using the delta–delta Ct method.

Western blotting

For ferritin protein detection on Western blot, the primary antibody used was rabbit anti-mouse FTH1 (D1D4; Cell Signaling Technology, Danvers, MA), at a concentration of 1:10,000, and the secondary antibody used was goat anti-rabbit IgG (Cell Signaling Technology), at a concentration of 1:5000. For ferroportin detection on Western blot, the primary antibody used was rat anti-mouse FPN (1C7; Amgen, Thousand Oaks, CA), at a concentration of 1:3300, and the secondary antibody used was rabbit anti-rat IgG (ab102213; Abcam, Cambridge, MA), at a concentration of 1:5000. For the actin protein loading control, mouse anti-actin antibody (A3854; Sigma-Aldrich), at a concentration of 1:50,000, was used. Chemiluminescent signal was detected using the ChemiDoc XRS+ System with Image Lab software (Bio-Rad).

Statistical analysis

Figure creation and statistical analysis was performed using Graph-Pad Prism 9.2.0 (San Diego, CA). Mouse data are presented as means \pm SDs, and *t* tests were used to compare group means. For non-normally distributed data, log transformation was applied prior to statistical analysis. *P* values < 0.05 were considered statistically significant.

RESULTS

Effects of FC in *Tmprss6* knockout mice

To assess the efficacy of FC in a high-hepcidin model, we evaluated the effects of 3 weeks of a 0.1% FC diet in *Tmprss6* knockout mice. TMPRSS6 functions to suppress hepcidin production. As expected, and as previously described,²⁰ compared to wild type (WT) littermates, the *Tmprss6* knockout mice had higher serum hepcidin concentrations and tended to have lower duodenum ferroportin protein levels (Figure 2a and b). Consistent with decreased enteral iron absorption, the *Tmprss6* knockout mice had decreased liver and serum iron concentrations (Figure 2c and d) and a microcytic anemia (Figure 2e–g), with a compensatory increase in serum erythropoietin (EPO) concentrations (Figure 2h). In this high-hepcidin model, FC increased duodenum ferroportin protein, liver iron, serum iron, mean corpuscular volume, and hemoglobin, with a compensatory decrease in serum EPO (Figure 2b–h).

Effects of FC in WT and *Tmprss6* knockout mice with CKD

To assess the efficacy of FC in even higher hepcidin models, we evaluated the effects of 3 weeks of a 0.1% FC diet in WT and *Tmprss6* knockout mice with adenine diet–induced CKD. Compared to non-CKD mice of the same genotype, both the WT and *Tmprss6* knockout mice with adenine-diet nephropathy had increased serum urea nitrogen; increased

serum hepcidin; increased liver iron, consistent with hepcidin-mediated iron sequestration; and a microcytic anemia with compensatory increases in serum EPO (Figure 3a–i). In these high-hepcidin CKD models, FC increased red blood cells and hemoglobin (Figure 3f and h). Also, as was observed in the non-CKD *Tmprss6* knockout mice, FC increased duodenum ferroportin protein in the CKD *Tmprss6* knockout mice (Figure 3c), consistent with the established mechanism of iron-induced, iron-responsive element binding protein (IRP)-mediated, de-repression of ferroportin translation.^{21–23}

Effects of FC in enterocyte-specific ferroportin knockout mice

To determine whether enteral FC absorption is dependent on ferroportin (i.e., absorbed via a transcellular, ferroportin-dependent pathway versus a paracellular, ferroportin-independent pathway), we assessed the effects of FC in a tamoxifen-inducible, enterocyte-specific ferroportin knockout murine model (Villin-Cre-ER^{T2}, *Fpn*^{fl^{ox}/fl^{ox}}). We first demonstrated that this model very effectively lowers duodenum ferroportin levels, resulting in decreased intestinal iron absorption and anemia. We injected mice with or without Villin-Cre-ER^{T2} with tamoxifen or sunflower oil vehicle control. Six weeks post-injection, control mice without Villin-Cre-ER^{T2} or that were not receiving tamoxifen had no change in duodenum ferroportin expression (Figure 4a and b) and no iron-deficiency anemia phenotype (Figure 4c–f). However, mice with Villin-Cre-ER^{T2} that received tamoxifen had an ~4000-fold decrease in duodenum *Fpn* mRNA expression (Figure 4a), undetectable duodenum FPN protein expression (Figure 4b), and increased duodenal enterocyte iron staining (Figure 4c)—consistent with decreased iron egress from the cells, decreased liver iron stores (Figure 4d), and microcytic anemia (Figure 4e and f).

Next, in a positive control experiment, we demonstrated that 3 weeks of a 1% FC diet can prevent iron-deficiency anemia when enterocyte ferroportin is present. In this experiment, 4-week-old WT mice were started on low-iron (4 ppm) diets. At 8 weeks of age, half of the mice had their diets supplemented with 1% FC. Mice were sacrificed 3 weeks later. The 1% FC diet increased liver iron stores (173 [44] vs. 7.7 [1.9] ug/g, $P < 0.001$; Figure 5a), increased serum iron concentrations (280 [37] vs. 166 [124] μg/dl, $P = 0.059$; Figure 5b), and prevented anemia (terminal hemoglobin 13.8 [0.7] vs. 7.6 [0.8], $P < 0.001$; Figure 5c), demonstrating that this iron regimen can effectively load WT mice.

We then tested whether 1% FC—effective at preventing iron-deficiency anemia (Figure 5)—could rescue the iron-deficiency anemia phenotype resulting from tamoxifen-induced enterocyte *Fpn* deletion (Figure 4). As before, tamoxifen-induced ferroportin deletion resulted in a dramatic decrease in duodenum ferroportin mRNA (Figure 6a) and protein (Figure 6b), causing iron-deficiency anemia (Figures 6c–i). Among the tamoxifen-induced (*Fpn* deleted) mice, 3 weeks of 1% FC did not increase liver iron (Figure 6e) or serum iron (Figure 6f), as it did in WT mice (Figure 5). Tamoxifen-induced (*Fpn* deleted) mice treated with or without FC had similar red blood cell counts, mean corpuscular volume, and hemoglobin (Hb: 8.9 [2.4] vs. 7.4 [2.1] g/dl, $P = 0.17$; Figure 6g–i), and FC did not prevent anemia, as it did in WT mice (Figure 5). These data suggest that enteral FC absorption is predominantly dependent on ferroportin, and that in this model, significant paracellular absorption does not occur.

Effects of FC in enterocyte-specific ferroportin knockout mice with CKD

Given that uremia may directly or indirectly affect enterocyte intercellular tight junction integrity,²⁴ possibly altering the potential for paracellular absorption, we repeated the experiment in the setting of CKD. As depicted in Figure 7, we used a 0.2% adenine diet to induce CKD,²⁵ then switched the mice to non-adenine diets with or without 1% FC, so as to avoid possible interactions between adenine and high dietary iron content. As in the non-CKD mice, tamoxifen markedly decreased duodenum ferroportin mRNA (Figure 8a) and protein (Figure 8b), resulting in decreased liver iron (Figure 8c). After 6 weeks of the adenine diet, serum urea nitrogen concentrations were elevated, and they did not differ between groups to be treated with versus without FC (Supplementary Figure S1A). Serum urea nitrogen concentrations decreased to similar degrees in mice treated with versus without FC (Figure 8d). In the uninduced CKD mice, FC treatment resulted in decreased duodenum ferroportin mRNA, but increased duodenum ferroportin protein, liver iron, and serum iron (Figure 8a–c and e; Supplementary Figure S1B). However, in the induced (*Fpn* deleted) CKD mice, FC treatment had no significant effect on liver or serum iron (Figure 8c and e; Supplementary Figure S1B). As expected, over time, the induced (*Fpn* deleted) mice became more anemic than the uninduced mice (Supplementary Figure S1C and D). FC did not increase red blood cell counts or hemoglobin in the uninduced or induced mice (uninduced delta Hb: -1.9 [2.5] vs. -1.7 [0.6] g/dl, $P = 0.89$; induced delta Hb: -2.3 [2.3] vs. -3.1 [2.3] g/dl, $P = 0.42$; Figure 8f and g), possibly reflecting the multifactorial etiology of anemia in this CKD model. Nevertheless, FC significantly improved iron status only in the uninduced CKD mice, suggesting that enteral FC absorption is predominantly dependent on ferroportin in this CKD model.

DISCUSSION

In clinical studies, FC has been shown to correct iron deficiency in patients with CKD and end-stage renal disease, which are states with high-hepcidin levels.^{5–8} In the setting of high circulating hepcidin concentrations, enteral ferroportin activity is decreased, engendering a hepcidin-mediated mucosal block to enteral iron absorption.⁹ The mechanisms by which FC may overcome this enteral absorptive block are unknown. One hypothesis is that the citrate moiety loosens intercellular tight junctions, facilitating paracellular, ferroportin-independent enteral iron absorption. We tested this hypothesis by assessing the effectiveness of FC in high-hepcidin/low-ferroportin models—with and without CKD—in which the transcellular iron absorptive pathway is nearly ablated or completely blocked.

In our first model, *Tmprss6* knockout mice without CKD, in which hepcidin levels are mildly elevated, FC improved iron status and increased hemoglobin concentrations. Similarly, in our WT and *Tmprss6* knockout models with CKD, in which hepcidin levels are markedly elevated, FC increased red blood cell count and hemoglobin. These data demonstrate the efficacy of FC in states with high hepcidin levels and are consistent with what has been observed in FC clinical studies; however, these models do not suggest what the mechanisms are by which FC overcomes the mucosal hepcidin block.

In these models, in which ferroportin remains intact, FC may be absorbed via a paracellular pathway, bypassing the hepcidin–ferroportin axis, or alternatively, may be absorbed via a

transcellular pathway, utilizing ferroportin. To evaluate the dependence of FC on enteral ferroportin, we used an inducible, enterocyte-specific ferroportin knockout murine model. This model is highly effective at nearly completely depleting enterocyte ferroportin protein, resulting in drastically reduced enteral iron absorption and severe iron-deficiency anemia, a phenotype that can be rescued by parenteral iron administration.²⁶ In this model, any substantial bypass of the canonical ferroportin-dependent pathway would be readily detectable.

In our non-CKD model, in the absence of enterocyte ferroportin, an FC dose that had been effective in WT mice did not improve iron status or rescue the iron-deficiency anemia phenotype. Small increases in red blood cell count and hemoglobin were not statistically significant, suggesting that enteral FC absorption is predominantly dependent on ferroportin, and arguing against extensive paracellular absorption. In the setting of CKD, uremia-associated factors potentially could increase gut permeability,²⁴ possibly loosening intercellular tight junctions and facilitating some degree of paracellular FC absorption. However, in our CKD model, FC significantly improved iron status in the presence of enterocyte ferroportin, but not in its absence. These data suggest that, even in the setting of CKD, enteral FC absorption is predominantly mediated by ferroportin transport and not possible paracellular pathways. In the uninduced CKD mice, FC treatment increased duodenum ferroportin protein, despite lower duodenum ferroportin mRNA expression, consistent with an established mechanism by which intracellular iron accumulation triggers IRP-mediated de-repression of ferroportin translation,^{21–23} thus facilitating cellular iron absorption and delivery to the circulation.

We performed 2 CKD experiments. Terminal average serum urea nitrogen and hemoglobin concentrations were similar between the WT CKD control diet group from the first experiment and the uninduced, untreated CKD group from the second experiment. However, in the first CKD experiment, WT mice treated with FC had a significant increase in hemoglobin, but in the second CKD experiment, the uninduced mice treated with FC did not have a significant increase in hemoglobin. The reason FC did not significantly increase hemoglobin in the uninduced mice, despite clearly improving iron status, is unclear; however, possible contributory factors include the multifactorial etiology of CKD anemia, the small sample sizes of uninduced mice, and the repeated phlebotomy in this experiment. An additional study limitation is that we used mouse models whose translatability to humans is not certain. Also, although robust, the evidence for the lack of significant paracellular absorption of FC is indirect.

In summary, in our high-hepcidin-level models, we observed beneficial effects of FC on iron and erythrocytic parameters, suggesting effective enteral iron absorption despite high hepcidin levels. To assess whether FC may bypass the mucosal hepcidin block via potential citrate-facilitated paracellular absorption, we evaluated an inducible, enterocyte-specific ferroportin knockout model, in the presence or absence of impaired kidney function. In these models, FC did not rescue the iron-deficiency anemia phenotype, demonstrating that enteral FC absorption is predominantly dependent on ferroportin, and suggesting that paracellular pathways likely do not constitute major routes of physiologic FC absorption.

Supplementary Material

Refer to Web version on PubMed Central for supplementary material.

DISCLOSURE

MRH and TG receive research support from Akebia Therapeutics Inc. All the other authors declared no competing interests.

REFERENCES

1. Block GA, Fishbane S, Rodriguez M, et al. A 12-week, double-blind, placebo-controlled trial of ferric citrate for the treatment of iron deficiency anemia and reduction of serum phosphate in patients with CKD Stages 3-5. *Am J Kidney Dis.* 2015;65:728–736. [PubMed: 25468387]
2. Yokoyama K, Hirakata H, Akiba T, et al. Ferric citrate hydrate for the treatment of hyperphosphatemia in nondialysis-dependent CKD. *Clin J Am Soc Nephrol.* 2014;9:543–552. [PubMed: 24408120]
3. Lewis JB, Sika M, Koury MJ, et al. Ferric citrate controls phosphorus and delivers iron in patients on dialysis. *J Am Soc Nephrol.* 2015;26:493–503. [PubMed: 25060056]
4. Yokoyama K, Akiba T, Fukagawa M, et al. A randomized trial of JTT-751 versus sevelamer hydrochloride in patients on hemodialysis. *Nephrol Dial Transplant.* 2014;29:1053–1060. [PubMed: 24376274]
5. Zaritsky J, Young B, Wang HJ, et al. Hepcidin—a potential novel biomarker for iron status in chronic kidney disease. *Clin J Am Soc Nephrol.* 2009;4:1051–1056. [PubMed: 19406957]
6. Ashby DR, Gale DP, Busbridge M, et al. Plasma hepcidin levels are elevated but responsive to erythropoietin therapy in renal disease. *Kidney Int.* 2009;75:976–981. [PubMed: 19212416]
7. Zaritsky J, Young B, Gales B, et al. Reduction of serum hepcidin by hemodialysis in pediatric and adult patients. *Clin J Am Soc Nephrol.* 2010;5:1010–1014. [PubMed: 20299375]
8. Troutt JS, Butterfield AM, Konrad RJ. Hepcidin-25 concentrations are markedly increased in patients with chronic kidney disease and are inversely correlated with estimated glomerular filtration rates. *J Clin Lab Anal.* 2013;27:504–510. [PubMed: 24218134]
9. Nemeth E, Tuttle MS, Powelson J, et al. Hepcidin regulates cellular iron efflux by binding to ferroportin and inducing its internalization. *Science.* 2004;306:2090–2093. [PubMed: 15514116]
10. Ganz T, Bino A, Salusky IB. Mechanism of action and clinical attributes of Auryxia® (ferric citrate). *Drugs.* 2019;79:957–968. [PubMed: 31134521]
11. Froment DP, Molitoris BA, Buddington B, et al. Site and mechanism of enhanced gastrointestinal absorption of aluminum by citrate. *Kidney Int.* 1989;36:978–984. [PubMed: 2601265]
12. Gupta A Ferric citrate hydrate as a phosphate binder and risk of aluminum toxicity. *Pharmaceuticals (Basel).* 2014;7:990–998. [PubMed: 25341358]
13. Folgueras AR, de Lara FM, Pendás AM, et al. Membrane-bound serine protease matriptase-2 (Tmprss6) is an essential regulator of iron homeostasis. *Blood.* 2008;112:2539–2545. [PubMed: 18523150]
14. Hanudel MR, Rappaport M, Gabayan V, et al. Increased serum hepcidin contributes to the anemia of chronic kidney disease in a murine model. *Haematologica.* 2017;102:e85–e88. [PubMed: 27884972]
15. Jia T, Olauson H, Lindberg K, et al. A novel model of adenine-induced tubulointerstitial nephropathy in mice. *BMC Nephrol.* 2013;14:116. [PubMed: 23718816]
16. Tamura M, Aizawa R, Hori M, et al. Progressive renal dysfunction and macrophage infiltration in interstitial fibrosis in an adenine-induced tubulointerstitial nephritis mouse model. *Histochem Cell Biol.* 2009;131: 483–490. [PubMed: 19159945]
17. Klinkhammer BM, Djurdjaj S, Kunter U, et al. Cellular and molecular mechanisms of kidney injury in 2,8-dihydroxyadenine nephropathy. *J Am Soc Nephrol.* 2020;31:799–816. [PubMed: 32086278]

18. Diwan V, Small D, Kauter K, et al. Gender differences in adenine-induced chronic kidney disease and cardiovascular complications in rats. *Am J Physiol Renal Physiol*. 2014;307:F1169–F1178. [PubMed: 25209863]
19. Kim A, Fung E, Parikh SG, et al. A mouse model of anemia of inflammation: complex pathogenesis with partial dependence on hepcidin. *Blood*. 2014;123:1129–1136. [PubMed: 24357728]
20. Finberg KE, Whittlesey RL, Fleming MD, et al. Down-regulation of Bmp/Smad signaling by *Tmprss6* is required for maintenance of systemic iron homeostasis. *Blood*. 2010;115:3817–3826. [PubMed: 20200349]
21. Darshan D, Wilkins SJ, Frazer DM, et al. Reduced expression of ferroportin-1 mediates hyporesponsiveness of suckling rats to stimuli that reduce iron absorption. *Gastroenterology*. 2011;141:300–309. [PubMed: 21570398]
22. Galy B, Ferring-Appel D, Becker C, et al. Iron regulatory proteins control a mucosal block to intestinal iron absorption. *Cell Rep*. 2013;3:844–857. [PubMed: 23523353]
23. Wilkinson N, Pantopoulos K. The IRP/IRE system in vivo: insights from mouse models. *Front Pharmacol*. 2014;5:176. [PubMed: 25120486]
24. Meijers B, Farré R, Dejongh S, et al. Intestinal barrier function in chronic kidney disease. *Toxins (Basel)*. 2018;10:298.
25. Schiavi SC, Tang W, Bracken C, et al. *Npt2b* deletion attenuates hyperphosphatemia associated with CKD. *J Am Soc Nephrol*. 2012;23:1691–1700. [PubMed: 22859851]
26. Donovan A, Lima CA, Pinkus JL, et al. The iron exporter ferroportin/Slc40a1 is essential for iron homeostasis. *Cell Metab*. 2005;1:191–200. [PubMed: 16054062]

Translational Statement

Ferric citrate (FC) has been shown to be an effective source of enterally absorbed iron in chronic kidney disease—a state with a high hepcidin level in which enterocyte ferroportin function is inhibited, limiting transcellular iron absorption. Here, in murine models with versus without impaired kidney function, we demonstrate that enteral FC absorption is dependent predominantly on conventional enterocyte iron transport by ferroportin, with any alternative pathways unable to compensate when ferroportin is inactivated. Therefore, in patients, enteral FC absorption is likely reliant on the regulated transcellular physiologic pathway, lessening concern about possible unregulated paracellular iron absorption.

Author Manuscript

Author Manuscript

Author Manuscript

Author Manuscript

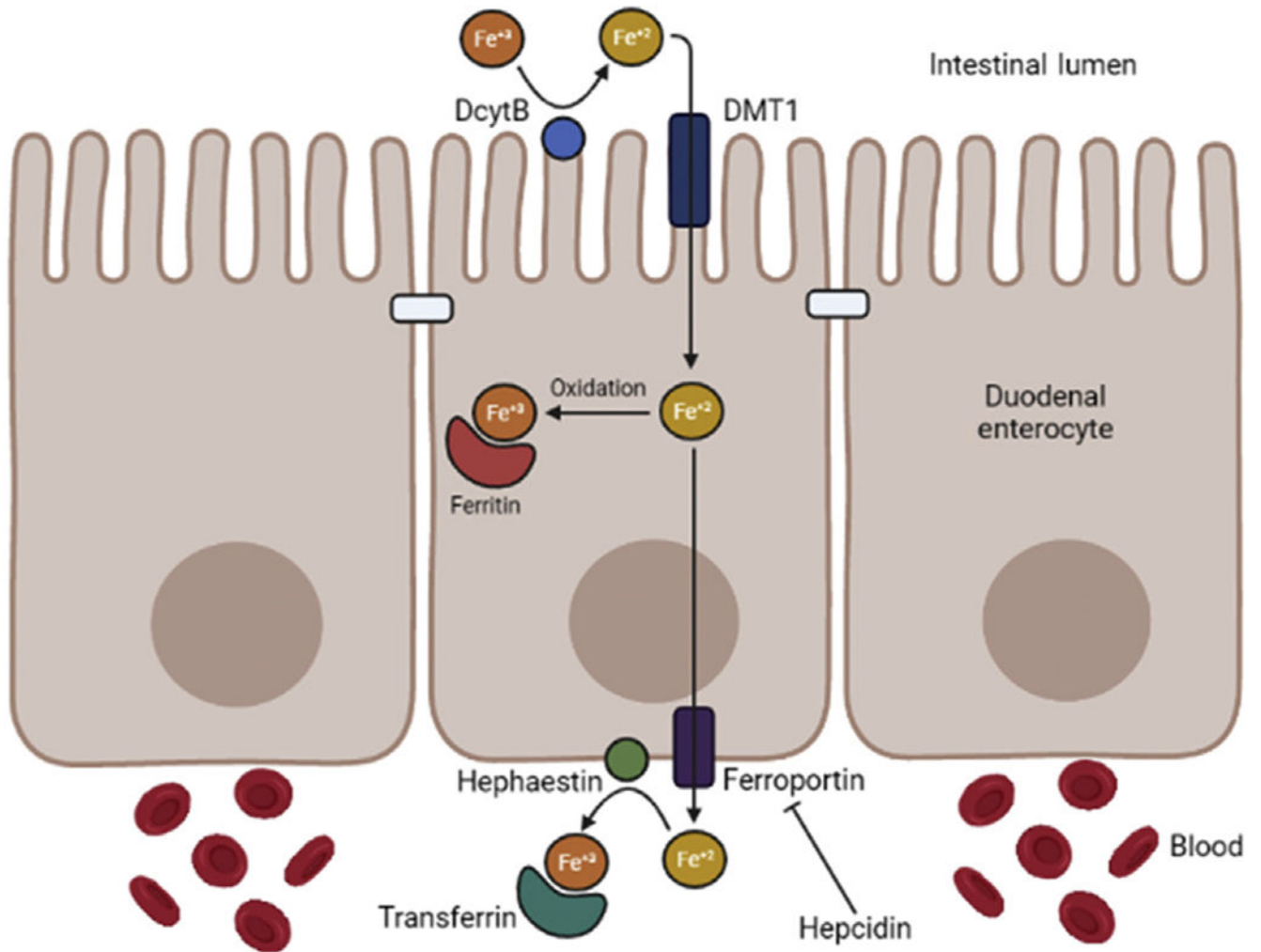


Figure 1 |. Mechanisms of enteral iron absorption.

DcytB, duodenal cytochrome B; DMT1, divalent metal transporter 1. Adapted from Ganz T, Bino A, Salusky IB. Mechanism of action and clinical attributes of Auryxia® (ferric citrate). *Drugs*. 2019;79:957–968.¹⁰ © The Author(s) 2019. CC BY-NC 4.0 (<http://creativecommons.org/licenses/by-nc/4.0/>). Created with [BioRender.com](https://www.biorender.com/).

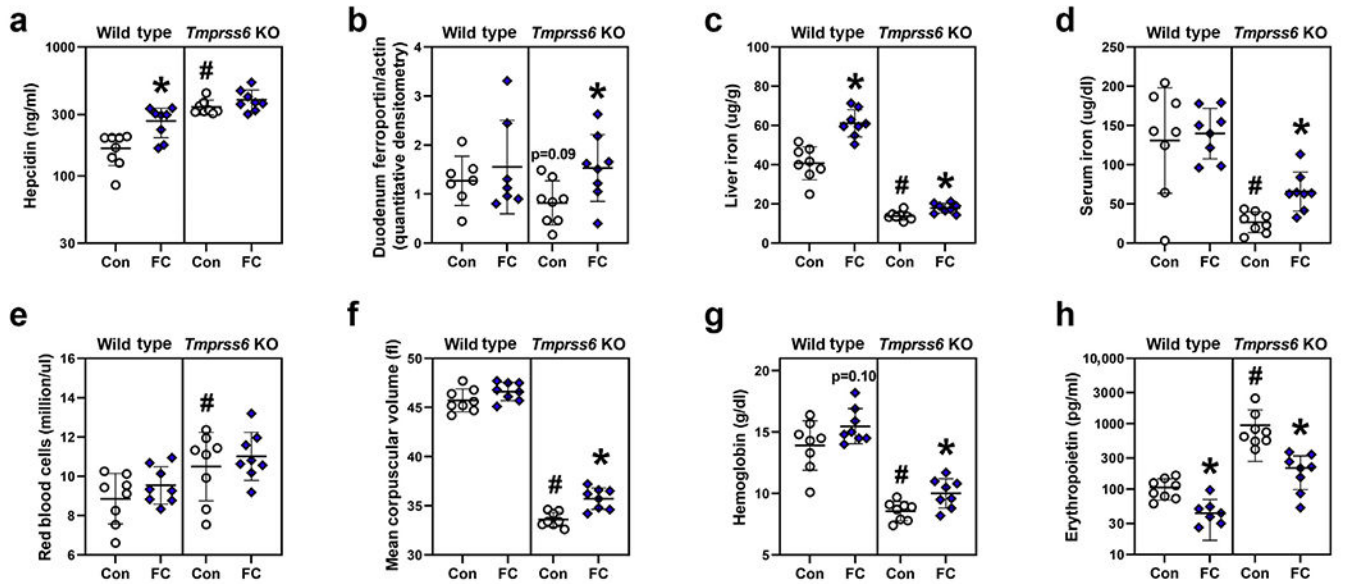


Figure 2 | Iron and erythropoietic parameters in wild type and *Tmprss6* knockout (KO) mice treated with versus without 0.1% ferric citrate (FC) added to the diet. Parameters measured include the following: (a) serum hepcidin; (b) duodenum ferroportin protein, assessed via Western blot quantitative densitometry; (c) liver iron; (d) serum iron; (e) red blood cell count; (f) mean corpuscular volume; (g) hemoglobin; and (h) serum erythropoietin. Logarithmic scales are used for (a) and (h). Data are presented as means and SDs. Unpaired *t* tests were used to compare groups. **P* < 0.05 for FC versus control (Con) diet within each genotype. #*P* < 0.05 for *Tmprss6* KO on control diet versus wild type on control diet. *n* = 8 mice per group.

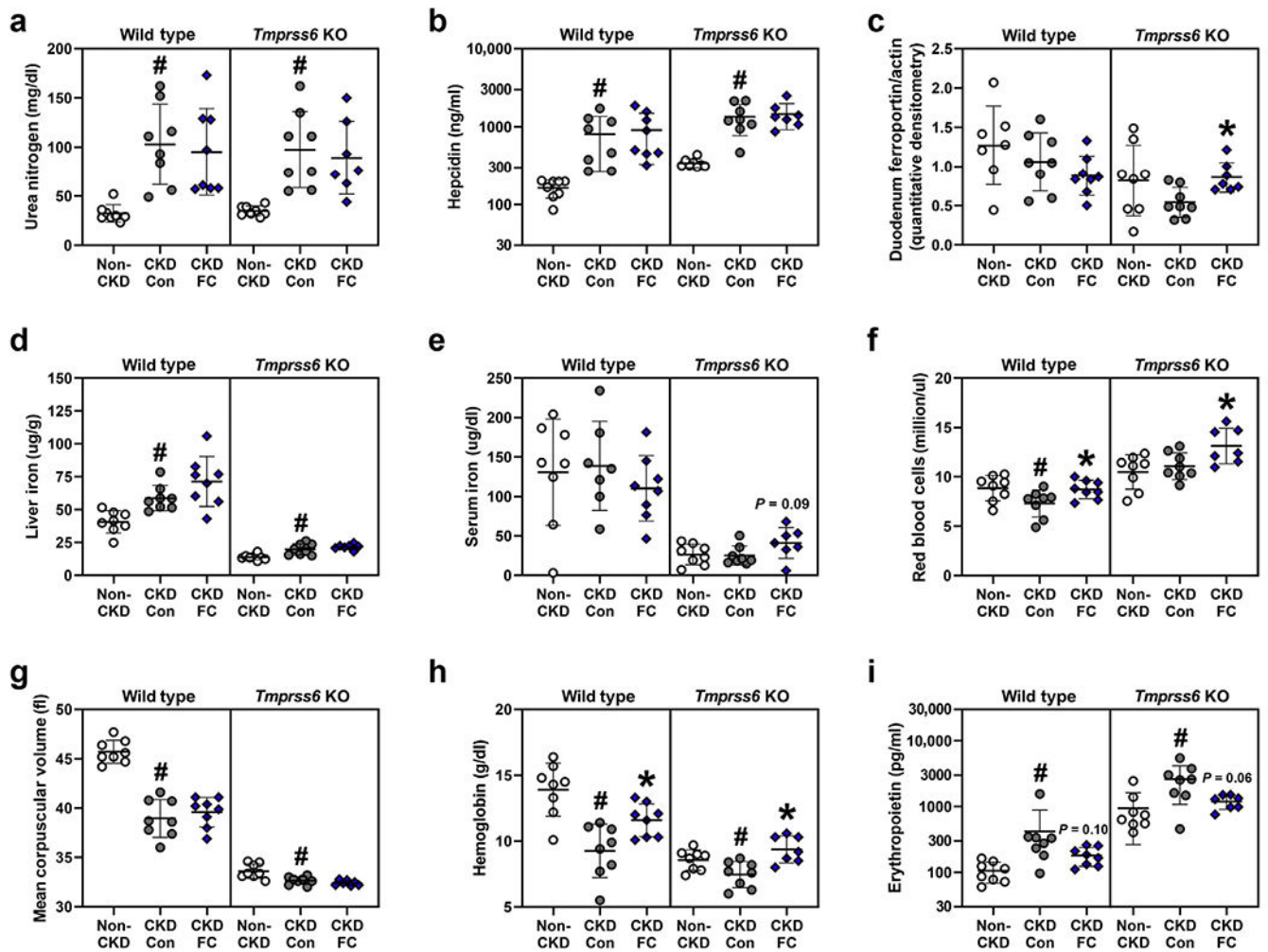


Figure 3 | Iron and erythropoietic parameters in wild type and *Tmprss6* knockout (KO) mice, with adenine diet-induced chronic kidney disease (CKD), treated with versus without 0.1% ferric citrate (FC) added to the diet.

Parameters measured include the following: (a) serum urea nitrogen; (b) serum hepcidin; (c) duodenum ferroportin protein, assessed via Western blot quantitative densitometry; (d) liver iron; (e) serum iron; (f) red blood cell count; (g) mean corpuscular volume; (h) hemoglobin; and (i) serum erythropoietin. Logarithmic scales are used for (b) and (i). Data are presented as means and SDs. Unpaired *t* tests were used to compare groups. * $P < 0.05$ for FC versus control (Con) diet within each genotype. # $P < 0.05$ for CKD on Con diet versus non-CKD on Con diet within each genotype. $n = 8$ mice per group. The non-CKD wild type and *Tmprss6* KO groups are the same Con groups presented in Figure 2.

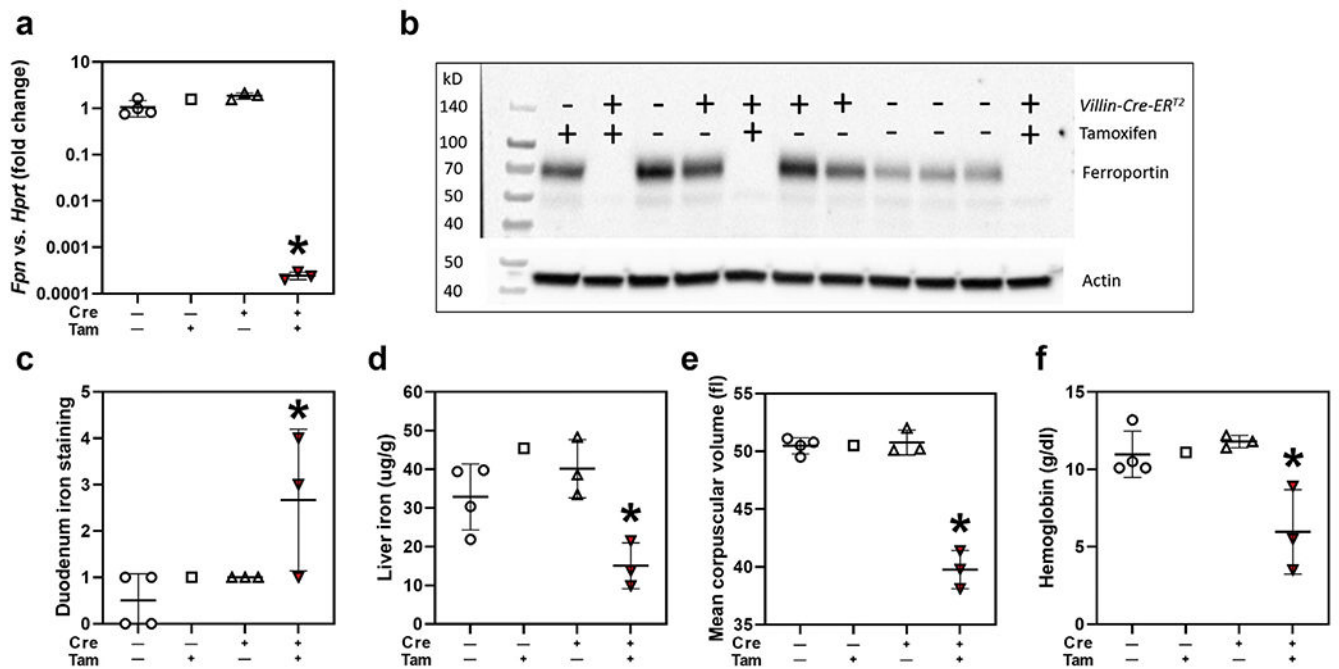


Figure 4 |. Characterization of the inducible, enterocyte-specific ferroportin (Fpn) knockout model.

Groups include the following: (i) $Fpn^{flx/flx}$ mice without Villin-Cre- ER^{T2} , not receiving tamoxifen (Tam; control group); (ii) $Fpn^{flx/flx}$ mice without Villin-Cre- ER^{T2} , receiving Tam; (iii) $Fpn^{flx/flx}$ mice with Villin-Cre- ER^{T2} , not induced with Tam; and (iv) $Fpn^{flx/flx}$ mice with Villin-Cre- ER^{T2} , induced with Tam. Parameters measured 6 weeks post-Tam injection include the following: (a) duodenum *Fpn* mRNA; (b) duodenum ferroportin protein, assessed via Western blotting; (c) duodenum iron staining; (d) liver iron; (e) mean corpuscular volume; and (f) hemoglobin. A logarithmic scale is used for (a). Data are presented as means and SDs. Unpaired *t* tests were used to compare groups. * $P < 0.05$ versus the control group.

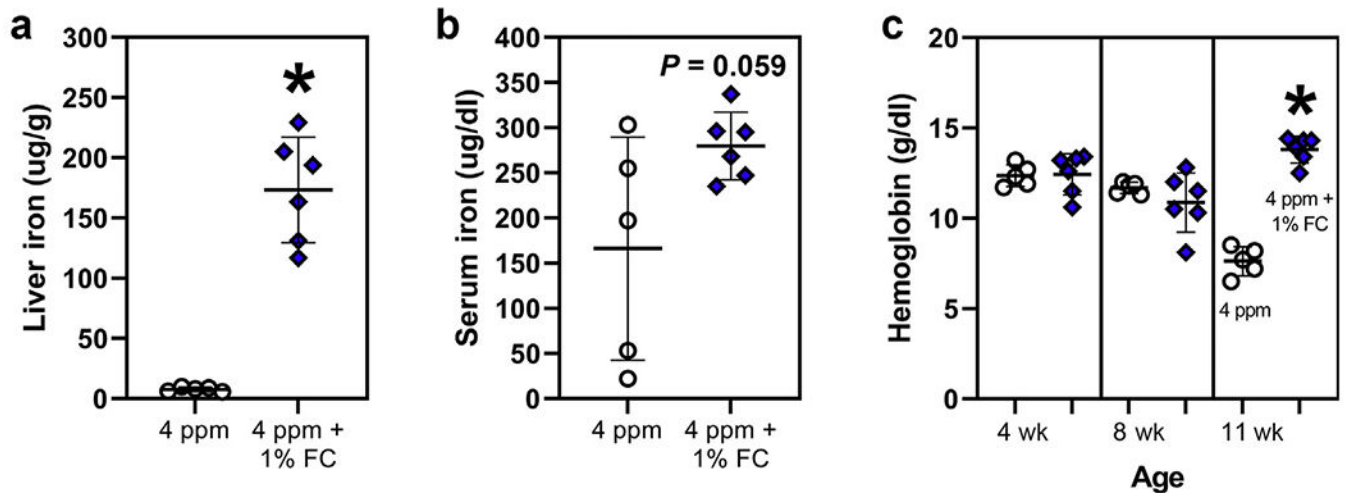


Figure 5 |. Prevention of iron-deficiency anemia by a 1% ferric citrate (FC) diet.

At 4 weeks of age, 11 uninduced Villin-Cre-ER^{T2}, Fpn^{flox/flox} (functionally wild type) mice were started on a low-iron (4 ppm) diet. At 8 weeks of age, 6 of the mice had their diets supplemented with 1% FC, and 5 of the mice did not. At 11 weeks of age, all mice were sacrificed. Parameters measured include the following: (a) terminal liver iron; (b) terminal serum iron; and (c) hemoglobin over time. Data are presented as means and SDs. Unpaired *t* tests were used to compare groups. * $P < 0.05$ versus untreated control group. $n = 5$ –6 mice per group.

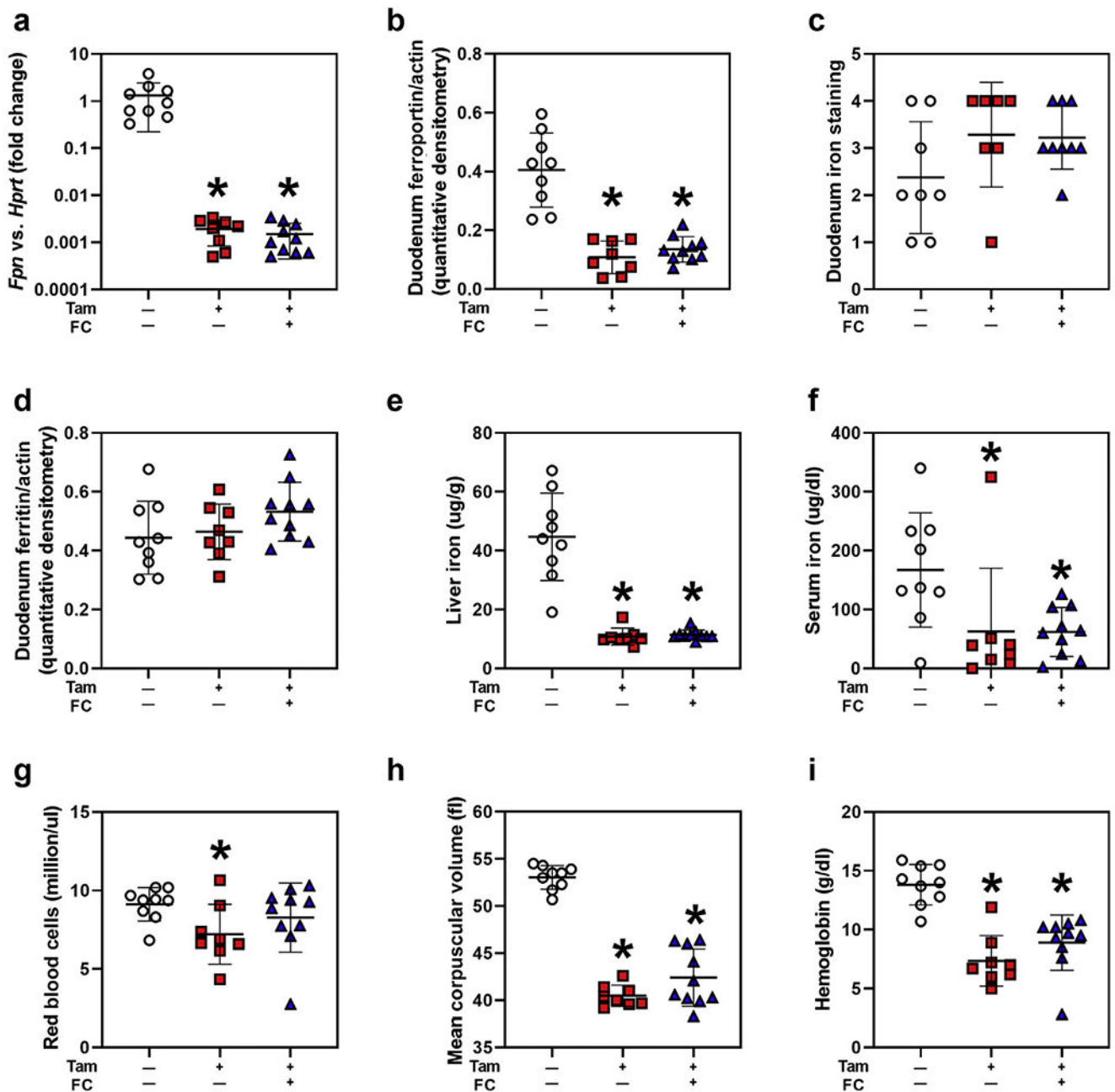


Figure 6 | Effects of a 1% ferric citrate (FC) diet in the inducible, enterocyte-specific ferroportin knockout model.

Groups include the following: (i) Villin-Cre-ER^{T2}, *Fpn*^{flx/flx} mice treated with vehicle (control group); (ii) Villin-Cre-ER^{T2}, *Fpn*^{flx/flx} mice induced with tamoxifen (Tam), not treated with FC; and (iii) Villin-Cre-ER^{T2}, *Fpn*^{flx/flx} mice induced with Tam, treated with 3 weeks of 1% FC diet supplementation. Parameters measured 7 weeks post-vehicle or post-Tam injection include the following: (a) duodenum *Fpn* mRNA; (b) duodenum ferroportin protein, assessed via Western blot quantitative densitometry; (c) duodenum iron staining; (d) duodenum ferritin protein, assessed via Western blot quantitative densitometry;

(**e**) liver iron; (**f**) serum iron; (**g**) red blood cell count; (**h**) mean corpuscular volume; and (**i**) hemoglobin. A logarithmic scale is used for (**a**). Data are presented as means and SDs. Unpaired *t* tests were used to compare groups. **P* < 0.05 versus the control group. *n* = 8–10 mice per group.

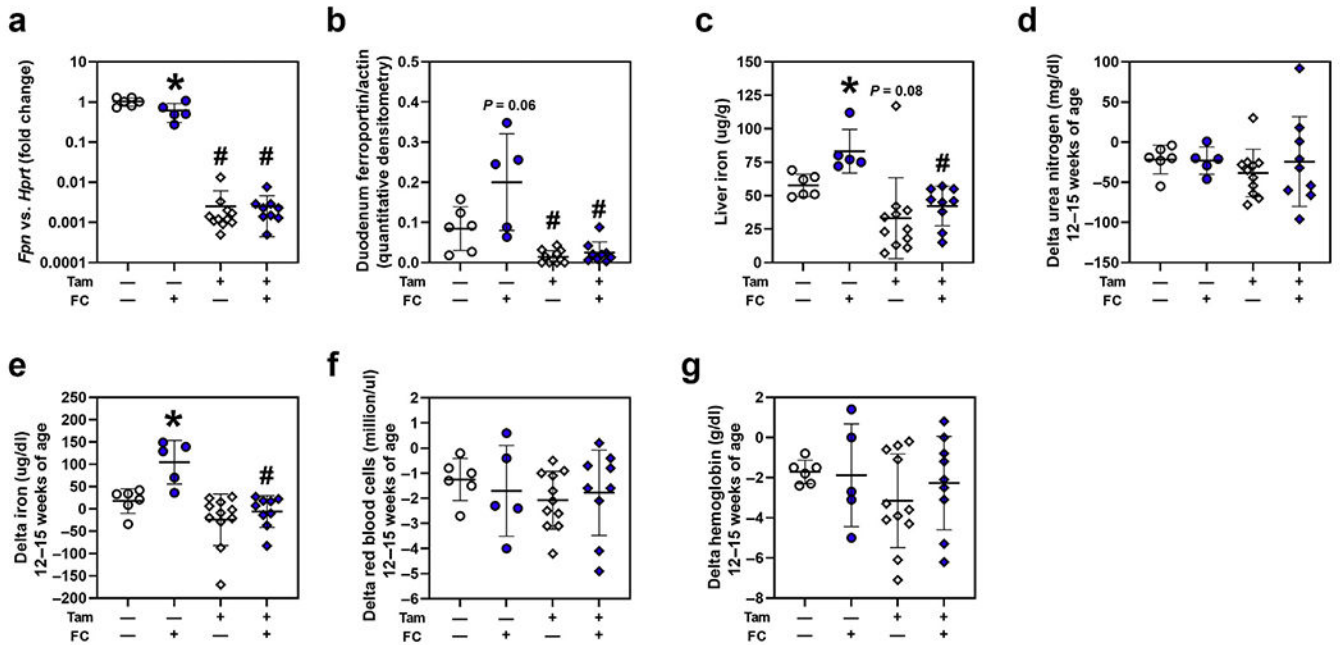


Figure 8 | Effects of a 1% ferric citrate (FC) diet in the inducible, enterocyte-specific ferroportin knockout model, with adenine diet-induced chronic kidney disease.

Villin-Cre-ER^{T2}, *Fpn*^{flox/flox} mice with adenine nephropathy were injected with tamoxifen (Tam) or sunflower oil vehicle control at 8 weeks of age, then administered diets with versus without 1% FC at 12–15 weeks of age. Parameters measured include the following: (a) duodenum *Fpn* mRNA; (b) duodenum ferroportin protein, assessed via Western blot quantitative densitometry; (c) liver iron; (d) change (delta) in serum urea nitrogen at 12–15 weeks of age; (e) change in serum iron at 12–15 weeks of age; (f) change in red blood cell count at 12–15 weeks of age; and (g) change in hemoglobin at 12–15 weeks of age. A logarithmic scale is used for (a). Data are presented as means and SDs. Unpaired *t* tests were used to compare groups. **P* < 0.05 for FC versus no treatment among uninduced or induced mice. #*P* < 0.05 for tamoxifen induction versus no induction among untreated or FC-treated mice. *n* = 5–11 mice per group.